Change in electrical resistivity due to icosahedral phase precipitation in Zr70Pd20Ni10 and Zr65Al7.5Cu7.5Ni10Ag10 glasses

doi: 10.1063/1.1394164

Change in electrical resistivity due to icosahedral phase precipitation in $Zr_{70}Pd_{20}Ni_{10}$ and $Zr_{65}Al_{7.5}Cu_{7.5}Ni_{10}Ag_{10}$ glasses

O. Haruyama,[a] and T. Miyazawa
Department of Physics, Faculty of Science and Technology, Science University of Tokyo, Noda, Chiba 278-8510, Japan

J. Saida
Inoue Supercooled Glass Project, ERATO, Japan Science and Technology Corporation, Sendai 980-0807, Japan

A. Inoue
Institute of Material Research, Tohoku University, Sendai 980-8577, Japan

(Received 28 February 2001; accepted for publication 14 June 2001)

The glass-to-icosahedral phase transformation in $Zr_{70}Pd_{20}Ni_{10}$ and $Zr_{65}Al_{7.5}Cu_{7.5}Ni_{10}Ag_{10}$ glasses was examined by the electrical resistivity measurement performed with a heating rate of 0.67 K/s. The resistivity increased with the promotion of icosahedral precipitation in $Zr_{70}Pd_{20}Ni_{10}$ glass. On the other hand, $Zr_{65}Al_{7.5}Cu_{7.5}Ni_{10}Ag_{10}$ glass exhibited the decrement of the resistivity according to the evolution of icosahedral phase. The latter was qualitatively explained by the drop of the resistivity of supercooled liquid phase due to the transfer of oxide atoms into the icosahedral phase. Also, the low temperature resistivity experiment showed that the conductivity of glassy and icosahedral phases might obey the weak localization model of conduction electrons. © *2001 American Institute of Physics.* [DOI: 10.1063/1.1394164]

Since the glass-to-icosahedral phase transformation was first reported in Al–Cu–V[1] amorphous alloy, the similar property was discovered in alloy systems such as Al–Mn–Si,[1] Pd–U–Si,[2] and Zr–Ti–Cu.[3] Recently, new Zr-based metallic glasses[4–8] have been also discovered to show similarly the glass-to-quasicrystal transformation. These Zr-based glasses were classified into two groups, one with a clear supercooled liquid region and another without it. The metallic $Zr_{70}Pd_{20}Ni_{10}$ glass belongs to the former and the $Zr_{65}Al_{7.5}Cu_{7.5}Ni_{10}Ag_{10}$ to the latter. A single icosahedral phase has been reported to evolve primarily from the glassy phase in $Zr_{70}Pd_{20}Ni_{10}$ glass and the supercooled liquid phase in $Zr_{65}Al_{7.5}Cu_{7.5}Ni_{10}Ag_{10}$ glass. Ultimately, the glass phase was transformed entirely to the icosahedral phase. The glass-to-quasicrystal transformation in $Zr_{65}Al_{7.5}Cu_{7.5}Ni_{10}Ag_{10}$ glass was found to occur in a polymorphous manner with the Avrami exponent nearly equal to 4.0.[7] For $Zr_{70}Pd_{20}Ni_{10}$ glass, the kinetics of *i*-phase precipitation is not reported but the mean composition in the icosahedral phase is deduced to be compatible with the glass phase because of a single *i* phase and the nano-structure of about 25 nm in size. The local structure of *i* phase formed in Zr-based glasses was reported to resemble that of corresponding metallic glass.[14] Thus this gives an opportunity to check and clarify the difference of electron transport property between glassy and icosahedral phases with almost the same chemical composition and the local structure. In this letter, we examine the change in the electrical resistivity associated with the glass-to-icosahedral phase transformation in $Zr_{70}Pd_{20}Ni_{10}$ and $Zr_{65}Al_{7.5}Cu_{7.5}Ni_{10}Ag_{10}$ glasses. Then, the low temperature conductivity for both glass and icosahedral phases is presented.

Master alloys with the composition of $Zr_{70}Pd_{20}Ni_{10}$ and $Zr_{65}Al_{7.5}Cu_{7.5}Ni_{10}Ag_{10}$ were produced by arc melting. Then ribbon samples with a cross section of $0.03\times1.5\,mm^2$ were prepared by melt-spinning technique. The amorphicity of samples was confirmed by x-ray diffraction and transmission electron microscopy (TEM). The glass-to-icosahedral phase transformation was examined by differential scanning calorimetry (DSC) at a heating rate of 0.67 K/s under the Ar gas flow. The electrical resistivity measurement was also carried out with the same experimental condition as in DSC. Additionally, the low temperature electrical resistivity experiment was performed from room temperature to 4.2 K for glass and icosahedral samples. The dc four-probe method was employed to measure the electrical resistivity. Then fine gold wires were spot welded to the samples as lead wires.

The DSC and resistivity curves of the as-quenched sample were shown in Fig. 1. The glass transition temperature T_g, the *i*-phase crystallization temperature T_{x1} and the crystallization temperature T_{x2}, in which they were defined from DSC curves, were almost the same as those reported previously.[7,8] The DSC signal increased gradually as the endothermic reaction due to glass transition extended in both glasses. In $Zr_{65}Al_{7.5}Cu_{7.5}Ni_{10}Ag_{10}$ glass, the supercooled liquid regime began at $T_{s.1}=680\,K$ after glass transition and then its DSC signal maintained a linear relationship with the temperature until T_{x1}. On the other hand, the *i*-phase precipitation occurred in a middle of glass transition for $Zr_{70}Pd_{20}Ni_{10}$ glass and a linear part on DSC curve did not appear. The resistivity of $Zr_{65}Al_{7.5}Cu_{7.5}Ni_{10}Ag_{10}$ glass continued to decrease with increasing the temperature until $T_{s.1}$ and hereafter increased until T_{x1}. We previously pointed

[a]Electronic mail: haruyama@ph.noda.sut.ac.jp

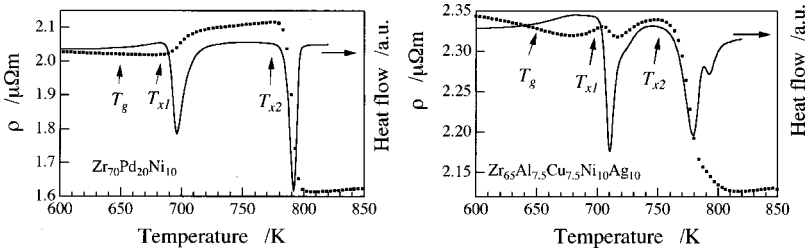

FIG. 1. DSC (solid line) and electrical resistivity (dotted line) curves with (a) $T_g=650$, $T_{x1}=685$ and $T_{x2}=775$ K for $Zr_{70}Pd_{20}Ni_{10}$ glass, and (b) $T_g=653$, $T_{x1}=705$ and $T_{x2}=753$ K for $Zr_{65}Al_{7.5}Cu_{7.5}Ni_{10}Ag_{10}$ glass.

out[12] that the temperature coefficient of resistivity (TCR) showed a negative value in the glassy solid region and then it turned to a positive one in the supercooled liquid region of $Zr_{60}Al_{25}Ni_{15}$ glass. Thus it is reasonable to consider that this mechanism acted similarly in $Zr_{65}Al_{7.5}Cu_{7.5}Ni_{10}Ag_{10}$ glass. It is concluded that *i*-phase crystallization of $Zr_{70}Pd_{20}Ni_{10}$ glass occurred on the way to supercooled liquid state, while the *i* phase of $Zr_{65}Al_{7.5}Cu_{7.5}Ni_{10}Ag_{10}$ glass transformed from the supercooled liquid phase. Then, the *i*-phase precipitation resulted in the opposite contribution to the resistivity of $Zr_{60}Pd_{20}Ni_{10}$ and $Zr_{65}Al_{7.5}Cu_{7.5}Ni_{10}Ag_{10}$ glasses. That is, the resistivity increased in the former and decreased in the latter along with the precipitation of the *i* phase. The TEM micrographs after finishing the *i*-phase crystallization were presented in Fig. 2. The diffraction patterns show the fivefold symmetry peculiar to icosahedral phase. The *i* phase formed shows the texture with nano-scaled grains of the average size of 25 and 45 nm for $Zr_{70}Pd_{20}Ni_{10}$ and $Zr_{65}Al_{7.5}Cu_{7.5}Ni_{10}Ag_{10}$ glasses, respectively. The amorphous phase was impossible to observe in these micrographs. The electron probe microanalysis showed that the chemical composition of the *i* phase almost coincided with the nominal compositions in $Zr_{65}Al_{7.5}Cu_{7.5}Ni_{10}Ag_{10}$ glass.[15] The similar analysis for $Zr_{70}Pd_{20}Ni_{10}$ glass is not already presented. However, it could be deduced from a single icosahedral phase formation in this glass that the shift of chemical composition in the icosahedral phase is likely slight. In order to compare with the electron transport of glassy and icosahedral phases, the low temperature resistivity was measured from room temperature to 4.2 K. To obtain a single *i* phase, $Zr_{70}Pd_{20}Ni_{10}$ and $Zr_{65}Al_{7.5}Cu_{7.5}Ni_{10}Ag_{10}$ glassy samples were annealed up to 730 and 740 K, respectively. The room temperature resistivity $\rho(300)$ and the corresponding TCR $d\rho/dT/\rho(300)$ are depicted in Table I for glassy and icosahedral phases. The low temperature electrical conductivity $\Delta\sigma=\sigma-\sigma_0$, where σ_0 expresses σ at 0 K obtained by extrapolation from a *T*-linear region, is calculated from the resistivity data and the result is presented in Fig. 3. Also, each σ_0 is summarized in Table I. The electrical conductivity showed the $T^{1/2}$ dependence between room temperature and about 90 K. Subsequently, the *T*-linear region appeared in the range from 90 to about 30 K. The *T*-linear region below $T=\Theta_D/3$ on the conductivity curve and the subsequent $T^{1/2}$ dependence in the upper region is frequently explained by the weak localization model of conduction electron,[9] where Θ_D denotes the Debye temperature. Following this theory, the $\Theta_D=270$ K deduced from the present experiment is reasonable. Also, the violation of *T*-linear law was frequently reported in the region below 30 K.[9] Then the typical $T^{1/2}$ law that appeared in Zr–Cu and Hf–Cu glasses was reported to be due to the electron–electron interaction in this temperature regime.[9] Similar temperature dependence is visualized definitely in both *i* phases. In glassy phases, however, the distinct $T^{1/2}$ dependence was not observed below about 30 K and the conductivity became larger than that predicted from this temperature dependence. Conclusively, the conductivity of glassy phase and *i* phase is explained by the same mechanism, the weak localization of conduction electron, at least above 30 K. In Al–Cu–V[10] and Al–Mg–Pd[11] amorphous

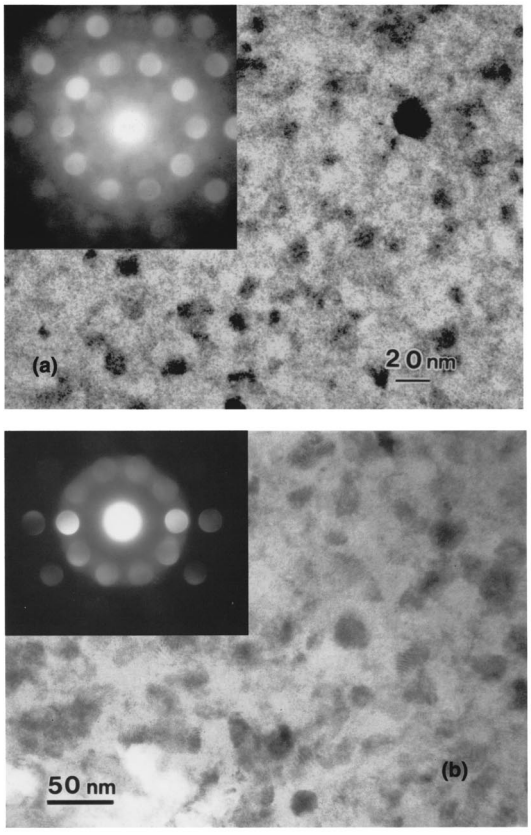

FIG. 2. Bright-field TEM image and nano-beam diffraction pattern for (a) $Zr_{70}Pd_{20}Ni_{10}$ icosahedral phase which was obtained by annealing at 700 K for 120 s, and (b) $Zr_{65}Al_{7.5}Cu_{7.5}Ni_{10}Ag_{10}$ one by annealing at 705 K for 60 s. The fivefold symmetry in the diffraction pattern peculiar to the icosahedral phase is visualized. No residual amorphous phase appeared in these micrographs.

TABLE I. Room temperature $\rho(300)$, $d\rho/dT/\rho(300)$ and the conductivity σ_0 at 0 K.

Alloy	Phase	$\rho(300)$ ($\mu\Omega$ m)	$d\rho/dT/\rho(300)$ ($\times10^{-4}$ K^{-1})	σ_0 (Ω^{-1} m^{-1})
	Glass	2.39 ± 0.12	-1.09 ± 0.02	397 890
$Zr_{65}Al_{7.5}Cu_{7.5}Ni_{10}Ag_{10}$	Icosahedral	2.41 ± 0.12	-0.33 ± 0.01	407 040
	Glass	2.07 ± 0.10	-0.90 ± 0.02	461 140
$Zr_{70}Pd_{20}Ni_{10}$	Icosahedral	2.22 ± 0.11	-1.00 ± 0.002	453 640

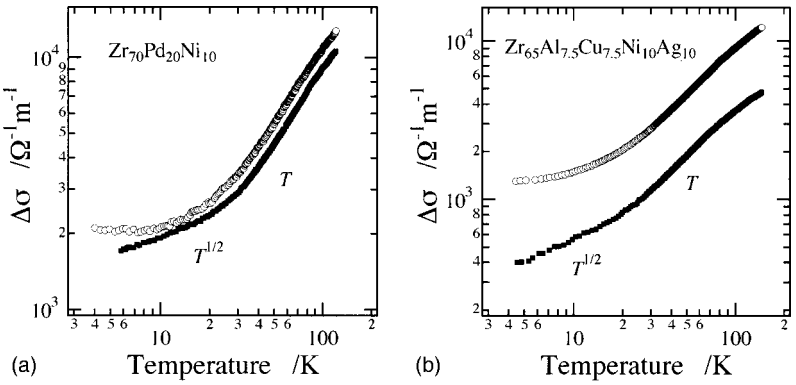

FIG. 3. Electrical conductivity $\Delta\sigma$ of glassy (○) and icosahedral (■) phases vs temperature for (a) $Zr_{70}Pd_{20}Ni_{10}$ alloy, and (b) $Zr_{65}Al_{7.5}Cu_{7.5}Ni_{10}Ag_{10}$ alloy.

alloys, where the single *i* phase was reported to evolve with almost the same composition as the amorphous phase, the electrical resistivity showed a larger value for the *i* phase than that for the amorphous phase. The $Zr_{70}Pd_{20}Ni_{10}$ glass exhibited the similar tendency. On the contrary, the resistivity of $Zr_{65}Al_{7.5}Cu_{7.5}Ni_{10}Ag_{10}$ glass decreased in the supercooled liquid region due to the promotion of *i*-phase crystallization. We reported previously that the resistivity of the $Zr_{60}Al_{25}Ni_{15}$ metallic glass was significantly influenced by the oxide contamination in the supercooled liquid region.[12] Then the positive TCR in the supercooled liquid region was explained by the decrement of the density of state $N(E_F)$ at Fermi energy E_F due to the formation of a bonding state between Zr and oxide atoms. The resistivity rise of $Zr_{65}Al_{7.5}Cu_{7.5}Ni_{10}Ag_{10}$ glass in the supercooled liquid region until T_{x1} suggests that the formation of Zr–O bonding occurred in this region. Although the detailed mechanism is not known yet, if the Zr–O bonding might be destroyed according to the formation of *i* phase, the resistivity would decrease along with the recovery of $N(E_F)$. It has been recently revealed by three-dimensional atom probe method[13] for Zr–Al–Cu glasses with the excess oxide content, each exhibiting the obvious supercooled liquid region, that the quasicrystalline phase is enriched in oxygen and its content is negligible in the amorphous phase. Therefore, the decrement of resistivity in early and intermediate stages of *i*-phase crystallization could be attributed to the fall of the resistivity of residual supercooled phase, which still occupied the major part of volume fraction in the sample. This suggests that the present consideration could be applied to other glass with the clear supercooled liquid region. We confirmed that the $Zr_{65}Al_{7.5}Cu_{7.5}Ni_{10}Pd_{10}$ glass exhibited the similar drop of the resistivity as *i*-phase crystallization proceeded. The later stage of *i*-phase precipitation, which appears as the small bump in the high temperature side of crystallization peak in the DSC curve, showed rather the increment of the resistivity. This could be attributed to the extended volume fraction of *i* phase with higher resistivity than the glassy phase. In the $Zr_{70}Pd_{20}Ni_{10}$ glass, the *i* phase precipitated from the glassy solid rather than the supercooled liquid. Then the mobility and the activity of oxide atom were presumably insufficient to form the *i* phase with a high content of oxygen. It is a common feature visualized in several alloys, showing the *i*-phase precipitation from the glassy solid region, that the resistivity is higher in the icosahedral phase than that in a glassy phase with identical composition. The indication[16] that the pseudo-Brillouin zone formed nearby Fermi surface results in the remarkable fall of density of state is suggestive to explain the high resistivity of *i* phase. However, that may not be the case for the present experiment, because the $\rho(300)$ of *i* phase in Zr-based glasses is only a few percent higher than that of the corresponding glass phase as shown in Table I.

[1] A. P. Tsai, A. Inoue, Y. Bizen, and T. Masumoto, Acta Metall. **37**, 1443 (1989).
[2] Y. Shen, S. J. Poon, and G. J. Shiflet, Phys. Rev. B **34**, 3516 (1986).
[3] V. V. Monokanov and V. N. Chebotnikov, J. Non-Cryst. Solids **117,118**, 789 (1990).
[4] U. Köster, J. Meinhardt, S. Roos, and H. Liebertz, Appl. Phys. Lett. **69**, 179 (1996).
[5] A. Inoue, T. Zhang, J. Saida, M. Matsushita, M. W. Chen, and T. Sakurai, Mater. Trans., JIM **40**, 1181 (1999).
[6] J. Saida, M. Matsushita, C. Li, and A. Inoue, Philos. Mag. Lett. **80**, 737 (2000).
[7] J. Saida, M. Matsushita, T. Zhang, A. Inoue, N. W. Chen, and T. Sakurai, Appl. Phys. Lett. **75**, 3497 (1999).
[8] J. Saida, M. Matsushita, and A. Inoue, Mater. Trans., JIM **41**, 543 (2000).
[9] M. A. Howson and D. Greig, Phys. Rev. B **30**, 4805 (1984).
[10] J. C. Holzer and K. F. Kelton, Acta Metall. Mater. **39**, 1833 (1991).
[11] U. Mizutani, Y. Yamada, T. Takeuchi, K. Hashimoto, E. Belin, A. Sadoc, T. Yamauchi, and T. Matsuda, J. Phys.: Condens. Matter **6**, 7335 (1994).
[12] O. Haruyama, K. H. Kimura, and A. Inoue, Mater. Trans., JIM **37**, 1741 (1996).
[13] B. S. Murty, D. H. Ping, and K. Hono, Appl. Phys. Lett. **76**, 55 (2000).
[14] E. Matsubara, T. Nakamura, M. Sakurai, M. Imafuku, S. Sato, J. Saida, and A. Inoue, in *2000 Proceedings of the Supercooled Liquid, Bulk Glassy and Nanocrystalline States of Alloys conference* (Material Research Society, Boston, 2000).
[15] A. Inoue, T. Zhang, N. W. Chen, and T. Sakurai, J. Mater. Res. **15**, 2195 (2000).
[16] P. A. Bancel and P. A. Heiney, Phys. Rev. B **33**, 7917 (1986).